Comptes rendus - Geoscience 351 (2019) 366–374

Contents lists available at ScienceDirect

Comptes rendus - Geoscience

www.journals.elsevier.com/comptes-rendus-geoscience

Petrology, Geochemistry

Petrogenesis and tectonic significance of mafic-ultramafic rocks from southwestern Yunnan, China

Qing Shi, Nianqiao Fang*

China University of Geosciences (Beijing), PR China

ARTICLE INFO

Article history:
Received 15 August 2018
Accepted 19 April 2019
Available online 11 June 2019
Handled by Marguerite Godard

Keywords:
Picrite
Mantle plume
Oceanic plateau
Palaeotethys

ABSTRACT

This study focuses on the mafic-ultramafic lavas of the Early Carboniferous outcrop in Mangxin, southwestern Yunnan, China. Picrites with 26–32 wt% MgO and a quenched texture are the most significant components of this rock association. This article divides the Mangxin picrites into two types. The mantle potential temperature (T_p) of these picrites is higher than the T_p range of mid-ocean ridges and reaches that of mantle plumes. According to their geochemical characteristics, type-1 picrites probably formed from the melting of the mantle plume head and were contaminated by the ambient depleted mantle, whereas type-2 picrites formed from the melting of mantle plume tails. These plume-related mafic-ultramafic rocks in Mangxin and the ocean island basalt (OIB)-carbonate rock associations in many areas of the Changning–Menglian belt provide significant evidence for the improvement of previous models of the Palaeotethyan oceanic plateau.

1. Introduction

Ultramafic lavas are generated by high degrees of partial melting (>10–15%) in the mantle (Herzberg and O'Hara, 2002). These lavas are an unusual type of Phanerozoic volcanics and have drawn the attention of many researchers (Arndt and Nisbet, 1982; Arndt et al., 2008; Herzberg and O'Hara, 2002). Several classic studies have revealed that ultramafic lavas such as picrites and komatiites may be produced by the fractional melting of a mantle plume (Arndt and Weis, 2002; Arndt et al., 1997). Hawaii is the most typical example of such a system: its intra-plate ocean island rock association of picrites, alkali, and tholeiitic basalts with high mantle potential temperatures indicate a plume origin (Herzberg and Asimow, 2015; Putirka et al., 2011). The Cretaceous komatiites of Gorgona Island were explained as products of the head of a mantle plume by Arndt et al. (1997) and Kerr et al. (1997). The picrites of Baffin Island and West Greenland were interpreted to be associated with the Tertiary Icelandic plume (Herzberg and O'Hara, 2002; Larsen and Pedersen, 2000). Although we cannot ignore picritic magmas that were produced by island-arc regimes, such as the Aleutians, Kamchatka, Solomon Islands, and Canada (Cameron and Nisbet, 1982; Kamenetsky et al., 1995; Milidragovic et al., 2016; Schuth et al., 2004), the preferred tectonic environment of ultramafic lavas is still related to mantle plumes based on the abnormal thermal conditions that are required by their high-Mg characteristics (Herzberg and O'Hara, 1998; Thompson et al., 2001).

Western Yunnan, China, is a region that has not attracted much research attention. Mafic and ultramafic lavas widely outcrop in this region, and the MgO contents of alkali basalts consistently reach 8–14%, while picrite pillows that outcrop at Xiaoheijiang have MgO contents of 35–40%. The picritic rock association that outcrops at Mangxin discussed in this article belongs to the Devonian to Triassic Palaeotethys orogenic belt, which is a different

* Corresponding author. China University of Geosciences (Beijing), No.29 Xueyuan Road, 100083, Beijing, PR China.
E-mail address: fangnq@yeah.net (N. Fang).

https://doi.org/10.1016/j.crte.2019.04.004

tectonic region from the Emeishan large igneous province (LIP). The picrites in Mangxin usually have an MgO content of 26–32% (loss on ignition (LOI)-free), and together with the local high-Mg accumulative peridotites and basalts, these rocks represent the largest and most diverse volcanic eruption on record in West Yunnan. Fang and Feng (1996) reported that these rocks represented the products of an ancient LIP in the Palaeotethys. Zhang and Zhu (1995) considered the Mangxin picrites to represent the failed accumulative rock that erupted in a mid-ocean ridge (MOR) environment. Zhong (1998) argued that these rocks were similar to Hawaiian picrites and were related to an oceanic island environment. Fang and Niu (2003) considered Mangxin picrites to have formed under high-temperature melting conditions. The purpose of this article is to utilize this rare geological record of Mangxin picrites, further analyse their characteristics, and discuss their petrogenesis and tectonic significance.

2. Geological background

Many previous studies have shown that the Changning–Menglian belt in western Yunnan, China, was the main basin of the Palaeotethyan archipelagic ocean (Fang et al., 1994; Liu et al., 1993; Zhong, 1998). Mangxin, the study area, is located at the southern end of the Changning–Menglian belt in China. This area contains abundant outcrops of Late Palaeozoic mafic-ultramafic pillow lavas, radiolarian chert, manganese rocks, and dolomitic pure carbonate rocks, thus providing an important window for understanding the evolution of the Palaeotethys. The samples were collected from the region to the south of Mangxin and included picrites, accumulative peridotites, and basalts. Detailed information about the geological background, sampling sites, analytical methods, and data can be found in the supplementary materials.

3. Petrological and geochemical characteristics of the samples

The picrites in Mangxin generally exhibit quenched textures in their matrices. These rocks can be divided into two different types based on their structures and compositions. The type-1 samples (MX01, MX02, MX03, and MX04) (Fig. 1a) are pillowed picrites with obvious porphyritic textures. Euhedral to subhedral olivine phenocrysts (0.1–3 mm) and few Cr-spinels are observed. The matrix mainly consists of skeletal-acicular clinopyroxenes and plagioclases as well as aphanitic alteration products. The average matrix compositions (LOI-free) of SiO_2 (47–48 wt%) and MgO (8–11 wt%) are similar to those of basaltic magma. Vesicles are visible (Fig. 1a). The type-2 samples (MX05 and MX06) are pillowed picrites with obvious porphyritic textures. Many euhedral olivines (0.1–2 mm) with clear edges and few Cr-spinels are observed. The matrix mainly consists of tiny feather-shaped pyroxenes and some aphanitic materials. No plagioclase is observed. The average matrix composition (LOI-free) of SiO_2 (41–43 wt%) and MgO (21–23 wt%) is similar to that of picritic magma. Fewer vesicles are visible (Fig. 1b). Although the classification of these two picrite types is similar to that reported by Fang and Niu (2003), the samples presented here were newly collected in 2013–2015 from different outcrops than those sampled by Fang and Niu (2003). The accumulative peridotites in this area (AP01, AP02) have been significantly altered. The olivines and clinopyroxenes form a cumulate texture. Most of the olivines are subhedral and have abundant fractures that are filled with serpentine and chlorite. The clinopyroxenes occur as anhedral grains in the gaps between olivines. Some Cr-spinels are visible. No quenched matrixes or vesicles are observed (Fig. 1c). The whole-rock compositions of the picrites and of the accumulative peridotites are similar. The SiO_2 contents of these ultramafic rocks are 43.56–47.50% (wt%) (LOI free), and the MgO contents reach

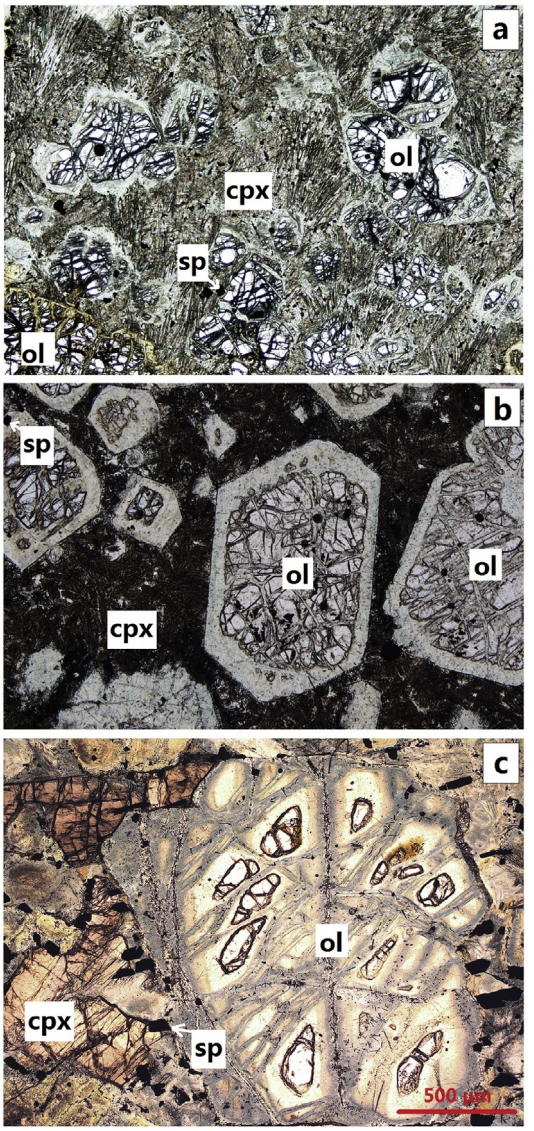

Fig. 1. Photomicrographs of picrite and accumulative peridotite samples from Mangxin under single-polarized light: (a) type-1 picrite; (b) type-2 picrite; (c) accumulative peridotite; ol, olivine; cpx, clinopyroxene; and sp, Cr-spinel.

26.35–32.31% (wt%). This high-Mg characteristic is similar to that of komatiites (MgO > 18%), but these samples did not contain "spinifex olivine" (Arndt and Nisbet, 1982). Therefore, we refer to them as "high-magnesium picrites" in the following discussion. This high-Mg characteristic indicates an accumulation of olivine.

The basalts in this area can also be divided into two types based on their chemical compositions. The high-Ti basalts have higher TiO_2 contents (3.17–3.87 wt%), but lower Al_2O_3 (12.93–14.94 wt%) and CaO (5.73–9.10 wt%) contents (LOI free). Their matrices consist of acicular plagioclases and granular clinopyroxenes, and the former are more prevalent than the latter. The acicular plagioclases are directionally arranged in some samples, indicating the flow of magma. Both plagioclase and clinopyroxene phenocrysts (0.5–1 mm) are observed. The low-Ti basalts have lower TiO_2 (1.07–1.82 wt%) contents, but higher Al_2O_3 (9.84–19.81 wt%) and CaO (8.22–14.73 wt%) contents (LOI free). Their matrices consist of tiny plagioclases and clinopyroxenes, and the latter are more prevalent than the former. Many clinopyroxene phenocrysts (0.5–2 mm) and vesicles are observed. A pillow structure is found in both types, confirming that they erupted in the same deep-sea environment as the picrites.

The SiO_2 content of the Mangxin basalts is positively correlated with MgO (Fig. 2a), whereas the SiO_2 and FeO contents in the Mangxin ultramafic rocks and the Al_2O_3 and TiO_2 contents in all of the samples are negatively correlated with the MgO content (Fig. 2a, b, 2c, and 2d). There is no obvious correlation between FeO and MgO in the Mangxin basalts (Fig. 2b). The ultramafic rocks can also be divided into two categories as basalts according to the TiO_2 contents: the type-1 picrites have lower TiO_2 contents (0.51–0.56 wt%), whereas the type-2 picrites and accumulative peridotites have higher TiO_2 contents (0.97–1.19 wt%) (Fig. 2d). The Mangxin samples have experienced some alteration, and the values of the loss on ignition (LOI) vary between 2.49 and 10.09 wt%. There is a negative correlation between LOI and Mg# in both the picrites and basalts, indicating that the alteration leads to a small decrease in Mg#.

The type-1 picrites are depleted in light rare-earth elements (REEs) and exhibit patterns similar to those of N-MORB; in particular, the curve of sample MX01 perfectly matches the curve of N-MORB, except for the negative Ce anomaly, which could be related to the alteration of olivine (Frisby et al., 2016; Niu, 2004). The type-2 picrites and accumulative peridotites are enriched in light REEs and

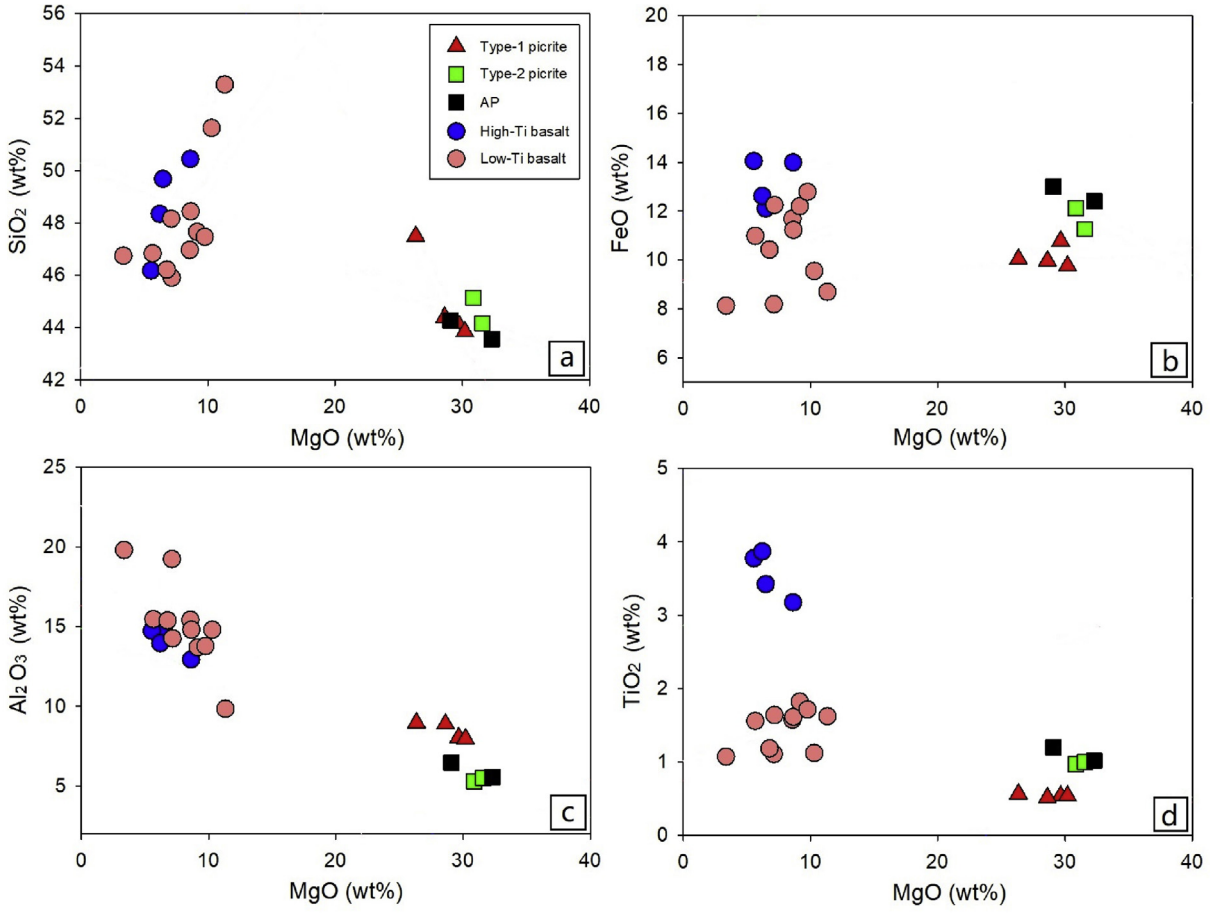

Fig. 2. Plots of certain major elements versus MgO for the Mangxin picrites, accumulative peridotites and basalts: (a) SiO_2 (wt%); (b) FeO^T (wt%); (c) Al_2O_3 (wt%); (d) TiO_2 (wt%) vs MgO (wt%). The total iron is expressed as FeO; AP, accumulative peridotites.

exhibit patterns similar to those of OIB, although their values are lower (Fig. 3a). The trace element spider diagrams also show that the patterns of the type-1 picrites are similar to those of N-MORB, but with more negative anomalies of Ta, Ti, Zr, and Hf, and positive anomalies of Pb. The curves of the type-2 picrites and accumulative peridotites are similar to those of OIB, except for the obvious negative anomalies of Ba, K, and Sr. These anomalies reflect the alteration of the samples (Fig. 3b). The two types of basalt in the Mangxin area have REE patterns similar to those of ultramafic rocks (Fig. 3c): the high-Ti basalts are enriched with light REEs and exhibit patterns similar to those of OIBs, whereas the low-Ti basalts have flat curves and exhibit patterns similar to those of E-MORB (more enriched in light REEs than N-MORB). The negative anomalies of Rb, K, and Sr in the high-Ti basalts also indicate alteration (Fig. 3d).

4. Discussion

4.1. Calculation of mantle potential temperature

In recent years, the topic of mantle plumes has attracted considerable attention. The concept of mantle potential temperature (T_p) was proposed to discuss the thermal anomalies in different regions of the mantle. According to different researchers, a clear distinction in T_p exists between MORs and hot spots affected by mantle plumes. The T_p values of MORs are 1280–1450 °C (Asimow et al., 2001; Herzberg and O'Hara, 2002; McKenzie and Bickle, 1988; McKenzie et al., 2005; Putirka, 2008). The T_p of Iceland is higher, at approximately 1480–1553 °C. The T_p of the Ontong Java Plateau is 1482–1534 °C. The T_p of Hawaii (Mauna Kea), which is widely regarded as a plume-affected oceanic island, reaches 1526–1549 °C. The T_p of Gorgona Island in the Caribbean LIP is 1539–1596 °C (Herzberg and Asimow, 2015; MacLennan et al., 2001). Thus, plume-associated regions generally have higher T_p values, we therefore hope to predict the probable plume influence by calculating the T_p of the Mangxin area.

To calculate the T_p, we must determine if the olivines represent mantle xenocrysts or are of magmatic origin. Only the latter can be used for the calculation. Most of the olivines in the Mangxin picrites are euhedral with clear edges and no zonal textures. According to Thompson and Gibson (2000), mantle olivines always have CaO contents below 0.1% (wt%), whereas magmatic olivines have CaO contents above 0.1% (wt%). Gavrilenko et al. (2016) showed that olivines that crystallized from a parental magma with high H_2O content (i.e. arc systems) always have low Ca contents (approximately 1000 ppm). The olivines in the Mangxin picrites generally have CaO contents of 0.2–0.3%

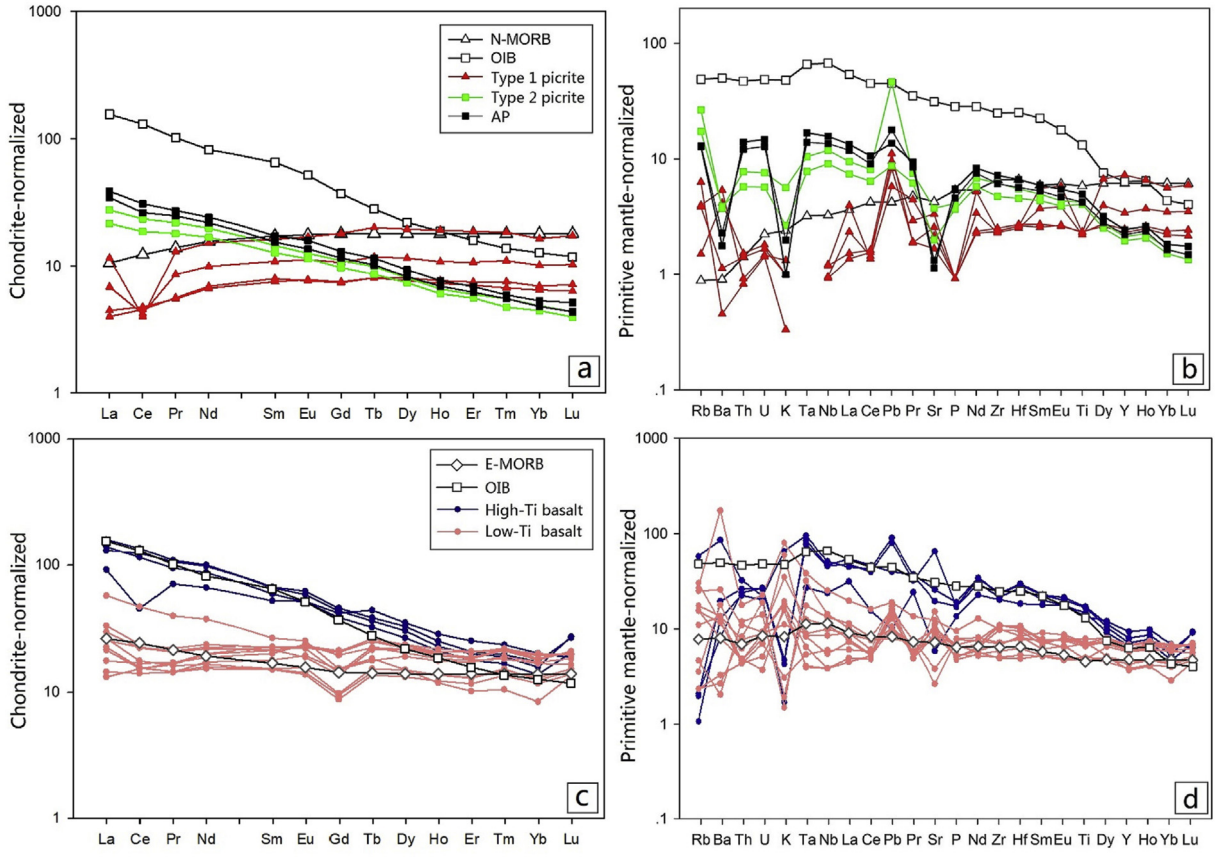

Fig. 3. Chondrite-normalized REE patterns and primitive mantle-normalized trace element diagrams of the Mangxin samples: (a) and (b), ultramafic rocks; (c) and (d) basalts. The normalization values, average OIB, N-MORB, and E-MORB compositions are from Sun and McDonough (1989).

(wt%), indicating an anhydrous magmatic origin. In addition, xenocrysts from the mantle always have kink bands because of the high pressure (Thompson and Gibson, 2000). No kink bands were observed in the Mangxin picrites, which also eliminates the possibility that these olivines are mantle xenocrysts.

Wan et al. (2008) provided a new Al-in-olivine thermometer to determine the minimum crystallization temperature (T_c). This thermometer is more reliable, because it is largely independent of the melt composition, H_2O content, and influences from olivine crystallization or accumulation. Coogan et al. (2014) improved this thermometer to expand its calibration range. The olivines in the Mangxin type-1 picrites generally have higher Al_2O_3 and Fo values than in the type-2 samples. Compared with those in other regions, the olivines in the type-1 picrites plot in a similar area as the olivines from the Siqueiros MORB and Gorgona komatiite in the Al_2O_3–Fo diagram, whereas the olivines in the type-2 picrites plot in a similar area as the olivines from the Hawaii basalt (Fig. 4a).

We used the improved Al-in-olivine thermometer from Coogan et al. (2014) to calculate the average T_c of the type-1 (1363 °C for MX01, 1417 °C for MX02 and 1332 °C for MX03) and type-2 picrites (1404 °C for MX05 and 1399 °C for MX06). The Fo–T diagram (Fig. 4b) of the olivines also shows the differences between the two types of Mangxin picrites. Coogan et al. (2014) contrasted the results of Al-in-olivine thermometry to those of other thermometers to assess the calculations' accuracy. Their results were consistent with the olivine crystallization temperatures calculated by Herzberg and O'Hara (2002). For example, the T_c of the Siqueiros MORB from Herzberg and O'Hara (2002) was 1277–1301 °C, which was only slightly higher than that from Al-in-olivine thermometry (1270 °C). Similar results were obtained for the Baffin Island basalts (1337–1445 °C vs 1408 °C) and Gorgona komatiites (1371–1457 °C vs 1435 °C). Thus, the results of Al-in-olivine thermometry are reliable. The calculated T_c values of the Mangxin picrites are higher than those of the Siqueiros MORB and similar to those of the Baffin Island basalts and Gorgona komatiites (Fig. 4b). Notably, the T_c from this approach is unlikely to exactly match the liquidus temperature, but the results should be very close to the liquidus temperature, and the difference may be within a few tens of degrees (Coogan et al., 2014).

For comparison, it is desirable to estimate the liquidus temperature from the MgO content of the liquid. The olivine-liquid Mg–Fe distribution coefficient (K_D) is relatively constant between 0.3 and 0.34, and increases with pressure (Putirka, 2005; Roeder and Emslie, 1970); therefore, we can estimate the MgO content of the liquid based on the composition of the olivine. For the Mangxin picrites, we used a K_D of 0.33 (Arndt and Nisbet, 1982) and the highest forsterite contents that were measured in olivines from each sample. The calculation was performed on the anhydrous whole-rock composition, assuming that the FeO content was constant during crystallization. Our calculation suggests that the parental magma of the Mangxin picrites had a MgO content of 20.72 wt% (MX01), 18.79 wt% (MX02), 16.82 wt% (MX03), 18.34 wt% (MX05), and 15.73 wt% (MX06). The amount of cumulus olivine in the Mangxin picrites varies from 30% to 50% according to a comparison with the whole-rock MgO composition. Then, the liquidus temperature, which is constrained by the relationship $T(°C) = 20 \times MgO + 1000$ (Arndt and Nisbet, 1982), varies from 1314 °C to 1414 °C, which is consistent with the value from the Al-in-olivine thermometer.

The T_p of the Mangxin picrites can be estimated by the approach of Putirka (2005) and the formula for the solidus of McKenzie and Bickle (1988). The T_p values for the type-1 (1465 °C for MX01, 1513 °C for MX02, and 1437 °C for MX03) and type-2 picrites (1502 °C for MX05 and 1497 °C for MX06) are calculated with a melt fraction in oceanic islands of 0.2 (Walter, 1998). The T_p of the ambient mantle, which feeds MOR basalt volcanism, is 1280–1450 °C, and the T_p of Phanerozoic intraplate basalts is 1450–1600 °C; these differences are attributed to anomalous thermal plumes (Asimow et al., 2001; Herzberg and O'Hara, 2002; Herzberg et al., 2010; McKenzie et al., 2005; Milidragovic et al., 2016; Putirka, 2008). The T_p of the Mangxin picrites is generally within the T_p range of mantle plumes (Table 1).

4.2. Information from high-field-strength elements

The contents and ratios of certain immobile high-field-strength elements (e.g., Th, Nb, Zr, Yb, Y, Hf, Ta, and Ti) are suitable for tracking the origin of old basalt samples because these elements are not affected by secondary alteration and do not change over time, unlike isotope ratios (Condie, 2005). The mantle is inhomogeneous, and several end-members have been divided based on their different isotope and trace element compositions. All types of mantle-derived magma can be explained by the mixing of these end-members. With the exception of PM (primitive mantle), Condie (2005) divided four different end-members of the oceanic mantle: DEP (deep plume component), EN (enriched component), REC (recycled component), and DM (shallow depleted mantle component). He compared samples from several plume-affected areas, such as the Caribbean Plateau, the Kerguelen Plateau, and Hawaii, and found that the basalts derived from plume heads had a mixed source of EN and DEP (plot between EN and DEP), whereas the basalts derived from plume tails were related to REC (plot near REC). However, one exception was observed: the picrites and komatiites that erupted on Gorgona Island were produced by a high degree of melting of the plume head (Révillon et al., 2000), although most of them plotted in the N-MORB area (near DM) in the Zr/Y–Nb/Y diagram. These rocks originated from an extremely depleted source that was unclear but similar to DM (Condie, 2005).

In the Zr/Y–Nb/Y diagram (Fig. 5a), most of the Mangxin basalts plot in the areas of OIBs and oceanic plateau basalts. Most of the high-Ti basalts plot near REC (related to plume tails), and the low-Ti basalts plot between EN and DEP (related to plume heads). Furthermore, the high-Ti basalts have higher TiO_2 contents and higher Ti/Y ratios (>500) than the low-Ti basalts, which is consistent with the high-Ti basalts being from a plume tail and the low-Ti basalts being from a plume head within the Emeishan LIP (Xu et al., 2004). The type-2 picrites and accumulative peridotites plot near high-Ti basalts and thus near REC,

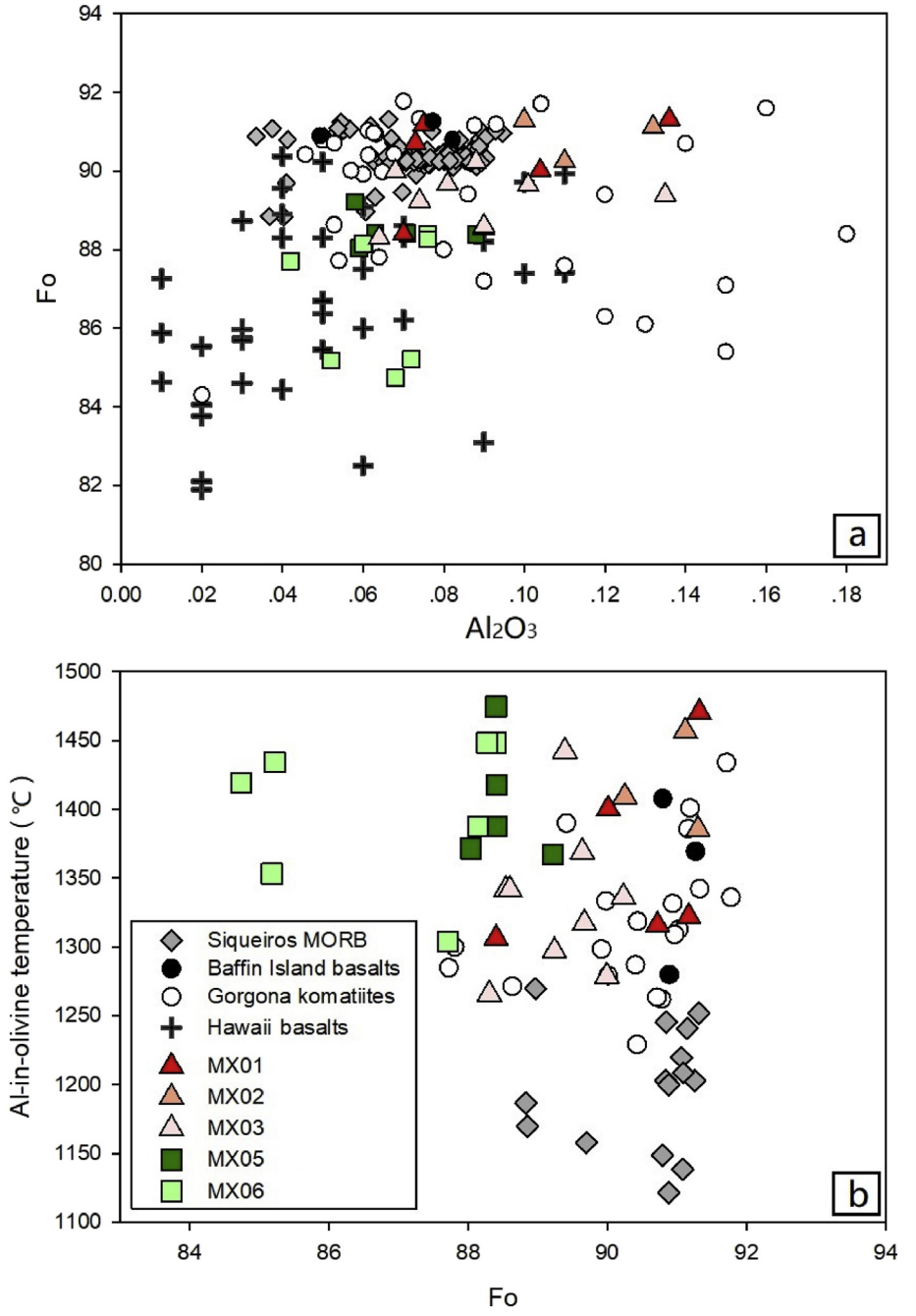

Fig. 4. Diagrams of Al-in-olivine temperature: (a) olivine Al_2O_3 content versus olivine Fo; (b) olivine Fo versus Al-in-olivine temperature. The Siqueiros data are from Putirka et al. (2011) and Coogan et al. (2014); the Baffin Island data are from Coogan et al. (2014); the Gorgona data are from Echeverría (1980) and Coogan et al. (2014); and the Hawaii data are from Rhodes (1995), Sobolev and Nikogosyan (1994) and Baker et al. (1996).

whereas most of the type-1 picrites plot near DM, which is similar to the characteristics of the picrites and komatiites from Gorgona.

In addition, the Nb/Yb–Th/Yb diagram (Fig. 5b) from Pearce (2008) shows similar results. Oceanic basalts, including OIB, E-MORB and N-MORB, are expected to plot within the MORB-OIB array in the Nb/Yb–Th/Yb diagram, whereas the lavas, with continental crust or subduction components, are expected to plot above the array. As shown in Fig. 5b, most of the Mangxin samples plot within the MORB-OIB array, suggesting that they are not arc-related. Most of the high-Ti basalts, type-2 picrites, and accumulative peridotites plot near OIB, whereas most of the low-Ti basalts plot near E-MORB, and the type-1 picrites plot near N-MORB; these plot locations are consistent with the characteristics of the REE patterns.

Table 1
Minimum crystallization temperatures and mantle potential temperatures of MORB, LIP, and the Mangxin picrites.

	Mangxin type-1 picrite			Mangxin type-2 picrite		MORB	LIP
	MX01	MX02	MX03	MX05	MX06		
T_c (°C)	1363	1417	1332	1404	1399	1270–1301	1337–1457
T_p (°C)	1465	1513	1437	1502	1497	1280–1450	1450–1600

The T_c and T_p values of MORB and LIP are summarized from Asimow et al. (2001), Coogan et al. (2014), Herzberg and O'Hara (2002), Herzberg et al. (2010), McKenzie and Bickle (1988), McKenzie et al. (2005), Milidragovic et al. (2016), Putirka (2008).

4.3. Speculation about the petrogenesis of the mafic-ultramafic rocks in Mangxin

According to the previous analysis, the T_p of the type-1 picrites calculated by the Al-in-olivine thermometer matched the T_p range of mantle plumes. These rocks had the same low-TiO_2 characteristic as the Mangxin low-Ti basalts, which may reflect a plume head origin. The characteristics apparent in the Zr/Y–Nb/Y diagram (near DM) and the Nb/Yb–Th/Yb diagram (near N-MORB) suggest that the type-1 picrites were contaminated by magma from a depleted source (i.e. ambient depleted mantle) during their eruption, which is also reflected in their depleted REE patterns. It is also possible that a depleted part of the plume head source existed; however, further studies are needed to discuss this possibility in detail. The T_p of the type-2 picrites was also within the T_p range of mantle plumes. The OIB-type REE and trace element patterns of accumulative peridotite were similar to those of the type-2 picrites, indicating that they had a similar magma source. The identical characteristics of the Mangxin type-2 picrites, accumulative peridotites and high-Ti basalts in the Zr/Y–Nb/Y and Nb/Yb–Th/Yb diagrams reflect their deep plume tail origin. It is also worth mentioning that high-Ti and low-Ti suites are typical classifications of continental flood basalts (CFBs); therefore, based on the archipelago setting, the possibility of continental crust contamination of the Mangxin basalts may also exist.

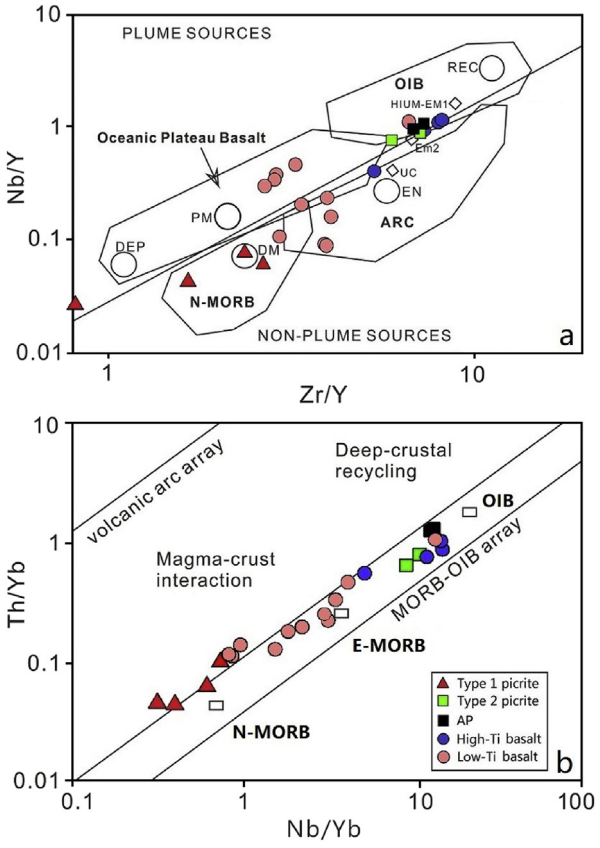

Fig. 5. High-field-strength element diagrams of Mangxin samples: (a) Zr/Y–Nb/Y diagram; (b) Nb/Yb–Th/Yb diagram: UC, upper continental crust; EM1 and EM2, enriched mantle sources; HIMU, high U/Pb source; PM, primitive mantle; DM, shallow depleted mantle; DEP, deep plume component; EN, enriched component; REC, recycled component; ARC, arc-related basalts; N-MORB, normal ocean ridge basalts; E-MORB, enriched ocean ridge basalts; OIB, oceanic island basalts (Condie, 2005; Pearce, 2008).

4.4. Speculation about a possible oceanic plateau in the Palaeotethys

To summarize, in the Mangxin area, (1) the formation of type-1 picrites and low-Ti basalts might have been related to the melting of the mantle plume head; (2) the formation of type-2 picrites and high-Ti basalts might have been related to the mantle plume tail (or core); and (3) the accumulative peridotites formed from a similar magma as the type-2 picrites in the magma chambers. Thus, we speculate that an oceanic plateau caused by a mantle plume might have been present in the basin of the Palaeotethys. This hypothesis is based on the geological background of the study area. The wide distribution of OIB-pure carbonate associations in the study area is notable. This kind of rock association outcrops in Yongde, Zhenkang, Gengma, Shuangjiang, Cangyuan, Lancang, and Menglian in western Yunnan, covers more than 40% of the Changning–Menglian belt and is often accompanied by radiolarian siliceous rocks, manganese rocks, and phosphate rocks. There have been numerous disputes about the tectonic environment represented by this rock association, such as rift, seamounts, island chain, arc or oceanic plateau. Based on the following facts.

(1) Most of the basalts are OIBs. The purity of the Early Carboniferous–Early Permian limestone overlying the basalts is very high (%wt > 96% $CaCO_3$). Their coexistence precludes a continental background, such as rift or arc (Liu et al., 1993).

(2) The age of the sedimentary interlayers in the volcanic rocks is Early Carboniferous (Tournaisian) (Feng et al., 1997; Zhang and Feng, 2002). Large-scale magmatic activity occurred during the same period, which precludes isolated seamounts and the possibility of forming seamount chains with plate drift. Fang et al. (1998)

speculated that there should be a large area of oceanic plateau in the main basin of the Palaeotethys, and the formation mechanism may be the role of large igneous province. This may currently be the most reasonable interpretation of the origin of the OIB–limestone association; it has gained the recognition of many researchers, but it also requires additional evidence. In particular, in the LIP system inferred by Fang, the ultramafic rocks are not clearly positioned. The monographic study of the Mangxin picrites, accumulative peridotites and two types of basalts undoubtedly provide significant evidence for the improvement of the previous model for the Palaeotethyan oceanic plateau.

5. Conclusions

(1) The mantle potential temperature (T_p) of type-1 and type-2 picrites in Mangxin as calculated by Al-in-olivine thermometry is 1437–1513 °C and 1497–1502 °C, respectively, which is within the T_p range of mantle plumes. The type-1 picrites formed from the melting of the mantle plume head. The type-2 picrites and accumulative peridotites formed from picritic magma that was produced by the mantle plume tail (or core), with the former erupting underwater, and the latter accumulating in magma chambers.

(2) The type-1 picrites had the REE, trace element and high-field-strength element characteristics of N-MORB, indicating possible contamination of the ambient depleted mantle and/or a relatively high melt fraction of the plume head. The type-2 picrites and accumulative peridotites exhibited the REE, trace element and high-field-strength element characteristics of OIB.

(3) The basalts in the Mangxin area could be divided into two types, based on the chemical compositions and the characteristics of their REE patterns and high-field-strength elements. The high-Ti basalts were similar to OIB and formed from the melting of the plume tail (or core), whereas the low-Ti basalts were similar to E-MORB and formed from the melting of the plume head.

(4) The existence of plume-related mafic-ultramafic rocks in Mangxin and the OIB-carbonate associations in many areas of the Changning–Menglian belt provide significant evidence for the improvement of the previous model for the Palaeotethyan oceanic plateau.

Acknowledgements

We are grateful to Dejan Milidragovic and Nicholas Arndt for performing a critical review of the manuscript. This work was supported by the National Natural Science Foundation of China (No. 41276047; No. 40876029).

Appendix A. Supplementary data

Supplementary data to this article can be found online at https://doi.org/10.1016/j.crte.2019.04.004.

References

Arndt, N.T., Lesher, C.M., Barnes, S.J., 2008. Komatiites. Cambridge University Press, Cambridge, UK.
Arndt, N.T., Nisbet, E.G., 1982. Komatiites. George Allen and Unwin, London.
Arndt, N.T., Weis, D., 2002. Oceanic plateaus as windows to the Earth's interior: an ODP success story. JOIDES J. 28 (1), 79–84.
Arndt, N.T., Kerr, A.C., Tarney, J., 1997. Dynamic melting in plume heads: the formation of Gorgona komatiites and basalts. Earth Planet. Sci. Lett 146 (1), 289–301.
Asimow, P.D., Hirschmann, M.M., Stolper, E.M., 2001. Calculation of peridotite partial melting from thermodynamic models of minerals and melts, IV. Adiabatic decompression and the composition and mean properties of mid-ocean ridge basalts. J. Petrol. 42, 963–998.
Baker, M.B., Sophie, A., Stolper, E.M., 1996. Petrography and petrology of the Hawaii Scientific Drilling Project lavas: inferences from olivine phenocryst abundances and compositions. J. Geophys. Res. Solid Earth 101 (B5), 11715–11727.
Cameron, W.E., Nisbet, E.G., 1982. Phanerozoic analogues of komatiitic basalts. In: Arndt, N.T., Nisbet, E.G. (Eds.), Komatiites. George Allen and Unwin, London, pp. 29–50.
Condie, K.C., 2005. High field strength element ratios in Archean basalts: a window to evolving sources of mantle plumes? Lithos 79, 491–504.
Coogan, L.A., Saunders, A.D., Wilson, R.N., 2014. Aluminum-in-olivine thermometry of primitive basalts: evidence of an anomalously hot mantle source for large igneous provinces. Chem. Geol. 368, 1–10.
Echeverría, L.M., 1980. Tertiary or Mesozoic komatiites from Gorgona island, Colombia: field relations and geochemistry. Contrib. Mineral. Petrol. 73 (3), 253–266.
Fang, N.Q., Feng, Q.L., 1996. Devonian to Triassic Tethys in Western Yunnan, China. China University of Geosciences Press, Wuhan, China.
Fang, N.Q., Feng, Q.L., Zhang, S.H., Wang, X.L., 1998. Paleo-tythes evolution recorded in changning–menglian belt, western Yunnan, China. C. R. Acad. Sci. Paris, Ser. IIa 326, 275–282.
Fang, N.Q., Liu, B.P., Feng, Q.L., 1994. Late Paleozoic and Triassic deep-water deposits and tectonic evolution of the paleo-tethys in the changning–menglian and lancangjiang belts, southwestern Yunnan. J. Southeast Asian Earth Sci. 9, 374–463.
Fang, N.Q., Niu, Y.L., 2003. Late Palaeozoic ultramafic lavas in Yunnan, SW China, and their geodynamic significance. J. Petrol. 44 (1), 141–157.
Feng, Q.L., Ye, M., Zhang, Z.J., 1997. Early Carboniferous radiolarians from western yunnan. Acta Micropalaeontol. Sin. 14 (1), 79–92.
Frisby, C., Bizimis, M., Mallick, S., 2016. Seawater-derived rare earth element addition to abyssal peridotites during serpentinization. Lithos 248, 432–454.
Gavrilenko, M., Herzberg, C., Vidito, C., Carr, M.J., Tenner, T., Ozerov, A., 2016. A calcium-in-olivine geohygrometer and its application to subduction zone magmatism. J. Petrol. 57 (9), 1811–1832.
Herzberg, C., Asimow, P.D., 2015. PRIMELT3 MEGA.XLSM software for primary magma calculation: peridotite primary magma MgO contents from the liquidus to the solidus. Geochem. Geophys. Geosyst. 16 (2), 563–578.
Herzberg, C., O'Hara, M.J., 1998. Phase equilibrium constraints on the origin of basalts, picrites, and komatiites. Earth Sci. Rev. 44, 39–79.
Herzberg, C., O'Hara, M.J., 2002. Plume-associated ultramafic magmas of Phanerozoic age. J. Petrol. 43, 1857–1883.
Herzberg, C., Condie, K., Korenaga, J., 2010. Thermal history of the Earth and its petrological expression. Earth Planet. Sci. Lett 292, 79–88.
Kamenetsky, V.S., Sobolev, A.V., Joron, J.L., Semet, M.P., 1995. Petrology and geochemistry of Cretaceous ultramafic volcanics from Eastern Kamchatka. J. Petrol. 36, 637–662.
Kerr, A.C., Tarney, J., Marriner, G.F., Nivia, A., Saunders, A.D., 1997. The Caribbean-Colombian Cretaceous igneous province: the internal anatomy of an oceanic plateau. In: Mahoney, J.J., Coffin, M.F. (Eds.), Large Igneous Provinces: Continental, Oceanic, and Planetary Flood Volcanism. American Geophysical Union, Washington, DC, pp. 123–144.
Larsen, L.M., Pedersen, A.K., 2000. Processes in high-Mg, high-*T* magmas: evidence from olivine, chromite and glass in Palaeogene picrites from West Greenland. J. Petrol. 41 (7), 1071–1098.
Liu, B.P., Feng, Q.L., Fang, N.Q., Jia, J.H., He, F.X., 1993. Tectonic Evolution of Palaeo-Tethys Poly-Island-Ocean in Changning–Menglian and Lancangjiang Belts, Southwestern Yunnan, China. J. China Univ. Geosci. vol. 18 (5), 529–539.
MacLennan, J., Kenzie, D.M., Gronvöld, K., 2001. Plume-driven upwelling under central Iceland. Earth Planet. Sci. Lett. 194 (1–2), 67–82.
McKenzie, D., Bickle, M.J., 1988. The volume and composition of melt generated by extension of the lithosphere. J. Petrol. 29, 625–679.

McKenzie, D.P., Jackson, J., Priestley, K., 2005. Thermal structure of oceanic and continental lithosphere. Earth Planet. Sci. Lett. 233, 337–349.
Milidragovic, D., Chapman, J.B., Bichlmaier, S., Canil, D., Zagorevski, A., 2016. H_2O-driven generation of picritic melts in the Middle to Late triassic Stuhini arc of the Stikine terrane, British Columbia, Canada. Earth Planet. Sci. Lett. 454, 65–77.
Niu, Y.L., 2004. Bulk-rock major and trace element compositions of abyssal peridotites: implications for mantle melting, melt extraction and post-melting processes beneath Mid-Ocean Ridges. J. Petrol. 45, 1–36.
Pearce, J.A., 2008. Geochemical fingerprinting of oceanic basalts with applications to ophiolite classification and the search for Archean oceanic crust. Lithos 100, 14–48.
Putirka, K.D., 2005. Mantle potential temperatures at Hawaii, Iceland, and the mid-ocean ridge system, as inferred from olivine phenocrysts: evidence for thermally driven mantle plumes. Geochem. Geophys. Geosyst. 6 (5), 1–14.
Putirka, K.D., 2008. Thermometers and barometers for volcanic systems. Rev. Mineral. Geochem. 69, 61–120.
Putirka, K.D., Ryerson, F.J., Perfit, M., Ridley, W.I., 2011. Mineralogy and composition of the oceanic mantle. J. Petrol. 52, 279–313.
Révillon, S., Arndt, N.T., Chauvel, C., Hallot, E., 2000. Geochemical study of ultramafic volcanic and plutonic rocks from Gorgona island, Colombia: the plumbing system of an oceanic plateau. J. Petrol. 41 (7), 1127–1153.
Rhodes, J.M., 1995. The 1852 and 1868 Mauna Loa picrite eruptions: clues to parental magma compositions and the magmatic plumbing system. Washington, DC. Am. Geophys. Union Geophys. Monogr. 92, 241–262.
Roeder, P.L., Emslie, R.F., 1970. Olivine-liquid equilibrium. Contrib. Mineral. Petrol. 29, 275–289.
Schuth, S., Rohrbach, A., Munker, C., Ballhaus, C., Garbe-Schonberg, C., Qopoto, C., 2004. Geochemical constraints on the petrogenesis of arc picrites and basalts, New Georgia Group, Solomon Islands. Contrib. Mineral. Petrol. 148, 288–304.
Sobolev, A.V., Nikogosyan, I.K., 1994. Igneous petrology of long-lived mantle plumes: the Hawaii (Pacific) and Réunion islands (Indian Ocean). Petrology 2 (2), 131–168.
Sun, S.S., McDonough, W.S., 1989. Chemical and isotopic systematics of oceanic basalts: implications for mantle composition and processes. Geol. Soc., Lond., Spec. Publ. 42 (1), 313–345.
Thompson, R.N., Gibson, S.A., Dickin, A.P., Smith, P.M., 2001. Early cretaceous basalt and picrite dykes of the southern Etendeka region, NW Namibia: windows into the role of the Tristan mantle plume in Paraná–Etendeka magmatism. J. Petrol. 42, 2049–2081.
Thompson, R.N., Gibson, S.A., 2000. Transient high temperatures in mantle plume heads inferred from magnesian olivines in Phanerozoic picrites. Nature 407 (6803), 502.
Walter, M.J., 1998. Melting of garnet peridotite and the origin of komatiite and depleted lithosphere. J. Petrol. 39, 29–60.
Wan, Z.H., Coogan, L.A., Canil, D., 2008. Experimental calibration of aluminum partitioning between olivine and spinel as a geothermometer. Am. Mineral. 93, 1142–1147.
Xu, Y.G., He, B., Chung, S.L., Menzies, M.A., Frey, F.A., 2004. The geologic, geochemical and geophysical consequences of plume involvement in the Emeishan flood basalt province. Geology 30, 917–920.
Zhang, F., Feng, Q.L., 2002. Early carboniferous radiolarians in phosphoric nodule from manxin, menglian, south-western yunnan. Acta Micropalaeontol. Sin. (1), 99–104.
Zhang, S.Q., Zhu, Q.W., 1995. Late Palaeozoic volcanic rocks in the Menglian region, southwestern Yunnan. Tethyan Geol. 19, 21–37.
Zhong, D.L., 1998. The Paleotethyan Orogenic Belt in Western Yunnan and Sichuan. China Science Publishing and Media Ltd., Beijing.